



Isolating Crucial Steps in Induction of Infective Endocarditis With Preclinical Modeling of Host Pathogen Interaction

Christian Schwarz¹, Verena Hoerr^{1,2}, Yasemin Töre¹, Vanessa Hösker¹, Uwe Hansen³, Hélène Van de Vyver⁴, Silke Niemann⁴, Michael T. Kuhlmann⁵, Astrid Jeibmann⁶, Moritz Wildgruber^{1,7} and Cornelius Faber^{1*}

¹ Translational Research Imaging Center, Department of Clinical Radiology, University Hospital Muenster, Muenster, Germany, ² Institute of Medical Microbiology, University Hospital Jena, Jena, Germany, ³ Institute of Musculoskeletal Medicine, University Hospital Muenster, Muenster, Germany, ⁴ Institute of Medical Microbiology, University Hospital Muenster, Muenster, Germany, ⁵ European Institute for Molecular Imaging, University of Muenster, Muenster, Germany, ⁶ Institute for Neuropathology, University Hospital Muenster, Muenster, Germany, ⁷ Klinik und Poliklinik für Radiologie, Klinikum der Universität München, Munich, Germany

OPEN ACCESS

Edited by:

Lisa Sedger,
University of Technology Sydney,
Australia

Reviewed by:

Emanuele Durante Mangoni,
University of Campania Luigi Vanvitelli,
Italy

Mark Dayer,
Taunton and Somerset NHS Trust,
United Kingdom

Tamara Sztynka,
University of Technology Sydney,
Australia

*Correspondence:

Cornelius Faber
faberc@uni-muenster.de

Specialty section:

This article was submitted to
Infectious Diseases,
a section of the journal
Frontiers in Microbiology

Received: 18 February 2020

Accepted: 25 May 2020

Published: 18 June 2020

Citation:

Schwarz C, Hoerr V, Töre Y, Hösker V, Hansen U, Van de Vyver H, Niemann S, Kuhlmann MT, Jeibmann A, Wildgruber M and Faber C (2020) Isolating Crucial Steps in Induction of Infective Endocarditis With Preclinical Modeling of Host Pathogen Interaction. *Front. Microbiol.* 11:1325. doi: 10.3389/fmicb.2020.01325

Animal models of *Staphylococcus aureus* infective endocarditis (IE), especially in rodents, are commonly used to investigate the underlying pathogenesis, disease progression, potential diagnostic approaches, and therapeutic treatment. All these models are based on surgical interventions, and imply valve trauma by placing a polyurethane catheter at the aortic root. While the influence of endothelial damage and inflammation on the induction of IE has been studied intensively, the role of the catheter, as permanent source of bacteremia, and the interplay with bacterial virulence factors during the formation of IE is poorly understood. In our study, we aimed at identifying which set of preconditions is required for induction and formation of IE: (1) tissue injury, (2) permanent presence of bacteria, and (3) presence of the full bacterial repertoire of adhesion proteins. We investigated the manifestation of the disease in different modifications of the animal model, considering different degrees of endothelial damage and the presence or absence of the catheter. In four infection models the induction of IE was assessed by using two bacterial strains with different expression patterns of virulence factors – *S. aureus* 6850 and Newman. *In vivo* magnetic resonance imaging showed conspicuous morphological structures on the aortic valves, when an endothelial damage and a continuous bacterial source were present simultaneously. Cellular and inflammatory pathophysiology were characterized additionally by histology, real-time quantitative polymerase chain reaction analysis, and bacterial counts, revealing strain-specific pathogenesis and manifestation of IE, crucially influenced by bacterial adherence and toxicity. The severity of IE was dependent on the degree of endothelial irritation. However, even severe endothelial damage in the absence of a permanent bacterial source resulted in reduced valve infection. The spread of bacteria to other organs was also dependent on the pathogenic profile of the infectious agent.

Keywords: endocarditis, foreign body, MRI, *Staphylococcus aureus*, mouse model

INTRODUCTION

Over the last years the incidence of *Staphylococcus aureus* (*S. aureus*) infective endocarditis (IE) has continuously increased (Bussani et al., 2019). Along with medical progress, intensive treatment conditions such as renal hemodialysis, immunosuppression, and long term indwelling central venous catheters, but also the application of modern cardiac device implants and valve prostheses constitute increasing sources of infection (Hoerr et al., 2018). *S. aureus* is one of the leading pathogens, as it adheres easily through its plethora of adhesins on the surface of implants and is able to form thick multilayered biofilms (Manandhar et al., 2018).

Diagnosis of IE is based on the four columns: clinical symptoms, laboratory parameters, imaging, and microbiology which mainly follow the major and the minor modified Duke criteria (Baddour et al., 2005). Especially with respect to imaging IE, echocardiography remains the gold standard (Habib et al., 2015). In addition to image-based diagnostics, rapid detection and identification of the causative pathogen is decisive for a timely and targeted therapy. Notably, despite correct puncture of a peripheral vein after sufficient disinfection, in up to 35% of the cases blood cultures remain negative and delay the diagnosis (Subedi et al., 2017). As a consequence of delayed diagnosis, complications such as cardiac failure, systemic embolism, abscesses, bleeding, and organ infarction lead to a mortality rate of 30% in patients with *S. aureus* IE (Habib et al., 2015). The formation of *S. aureus* IE implies a series of different host and pathogen factors and can be induced through different pathogenic pathways (Werdan et al., 2014). Frequently the bacterial infestation of the valve is mediated by the two fundamental physiological conditions: endothelial damage of the cardiac valves and circulating bacteria (Angrist, 1963; Werdan et al., 2014). Mechanical trauma of the endothelium results in a rapid fibrinogen-fibrin network with platelet deposition which represents an ideal condition for *S. aureus* to adhere to the impaired cardiac valve. Subsequent interaction between immune cells, platelets, and bacteria as well as cytokines regulates the further growth and development of cardiac valve vegetations (Bancsi et al., 1996; Kobayashi et al., 2015).

To further advance therapeutic and preventive regimens and measures, different animal models of IE have been proposed in the past based on dogs (Highman et al., 1956), horses (Else and Holmes, 1972), pigs (Jones, 1969; Jones, 1982; Johnson et al., 1986), opossums (Rowlands et al., 1970), rabbits (Durack and Beeson, 1972; Durack et al., 1973), and rodents such as rats (Héraïef et al., 1982; Baddour et al., 1984; Gupta et al., 2013; Li et al., 2016) and mice (Gibson et al., 2007; Ring et al., 2014; Liesenborghs et al., 2019). All models depend on similar interventions. In the first instance a mechanical irritation and damage of the endothelium of the cardiac valves is induced by a polyethylene catheter, followed by a hematogenous *S. aureus* infection, providing circulating bacteria which have the capability to adhere to the harmed tissue (Moreillon et al., 2002). In most of the animal studies the catheter remains in place on the cardiac valves during progression of IE until the animal

is sacrificed. The presence and underlying role of the catheter during the infection is, however, controversially discussed in pertinent literature, as the catheter representing foreign material rather mimics the infection of a valve prostheses than of naïve valves (Sande and Zak, 1999).

Thus, within the frame of our study we systematically investigated the influence of the degree of valvular tissue damage, the presence of foreign material, as well as the different virulence profiles on the induction of *S. aureus* IE. In four different mouse models of IE with different modifications of valvular damage and catheter placement, two different *S. aureus* infections were examined using the strains 6850 and Newman. Magnetic resonance imaging (MRI) was used to depict the manifestations of bacterial vegetation on the valves, histology to confirm tissue damage and bacterial presence, colony forming units (CFU) counts to quantify bacterial distribution and burden, and clinical scores to represent the overall disease severity.

MATERIALS AND METHODS

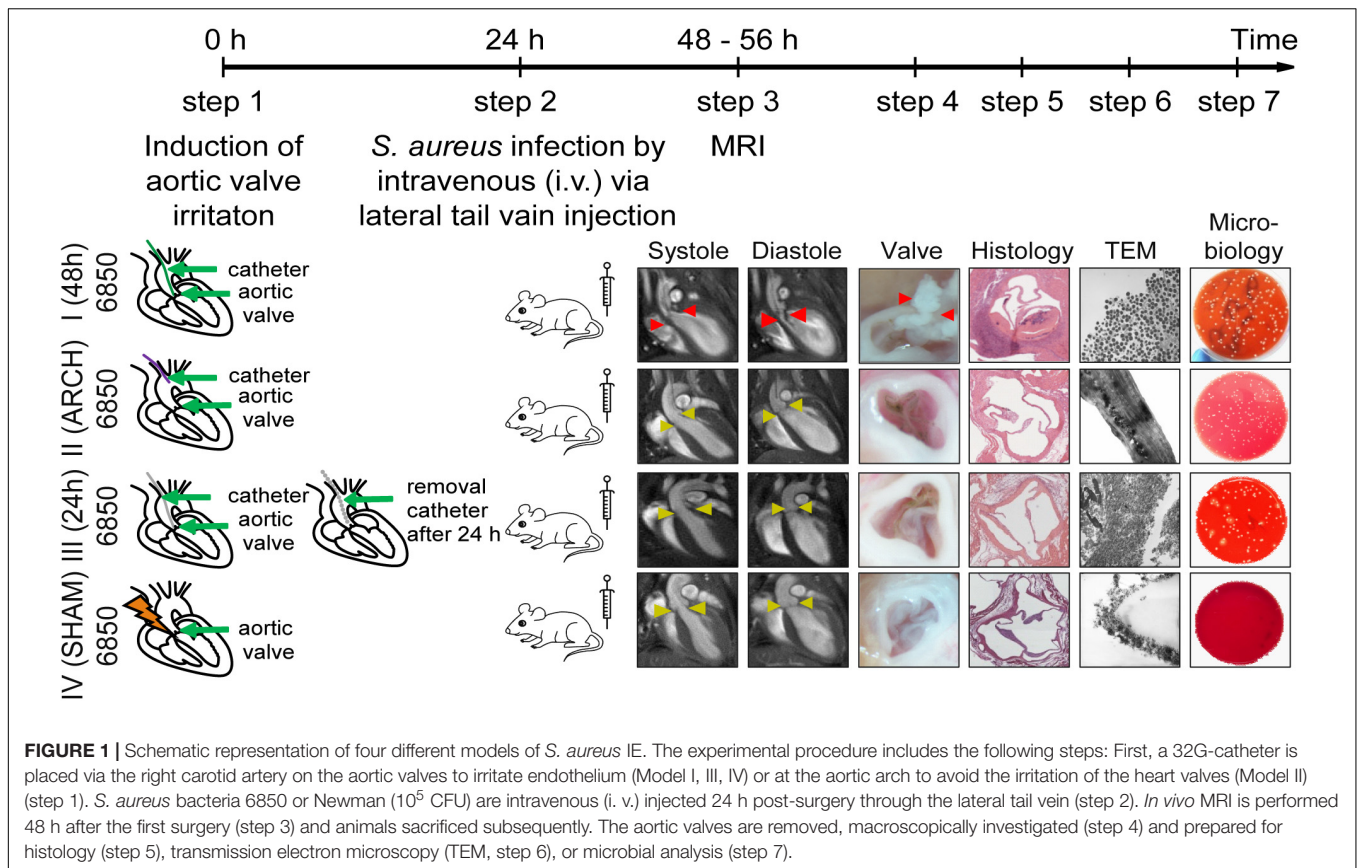
Mouse Model of *S. aureus*-Induced Infective Endocarditis

Female C57BL/6 mice ($n = 144$) with a body weight of 16–25 g (average weight: 21.5 ± 1.7 g) and an age of 8–12 weeks were used in this study.

For the induction of *S. aureus* IE, a surgical intervention was performed prior to the infection as described previously (Ring et al., 2014). A 32-G polyurethane catheter (13 mm of the tube were cut and heat-sealed at both ends) was placed via the right carotid artery at the aortic root to irritate the aortic valve. The aortic valves were reliably reached by slowly advancing the catheter until the vibration was induced by the fast moving aortic valves. An inoculation with *S. aureus* 6850 or Newman was performed 24 h post catheter placement by intravenous (i. v.) injection through the tail vein (see **Figure 1**).

Our study included 13 groups of animals comprising a naïve control group and four different surgical models that were each injected via the tail vein with either *S. aureus* 6850, *S. aureus* Newman, or phosphate-buffered saline (PBS; MOCK groups) 24 h after surgical intervention. The four interventions differed in site and duration of catheter placement (see **Figure 1**):

- Model I: The catheter was placed directly on the aortic valves for 48 h and was present during the whole time of infection. This model combined permanent valve damage with permanent bacteremia due to adherent bacteria on the catheter during progression of IE.
- Model II: The catheter was placed for 48 h in the aortic arch without damaging the aortic valve but was present during the whole time of infection, representing a bacterial source and thus permanent bacteremia. To put the catheter in the aortic arch, the catheter was cut to a length of 1 cm to avoid irritation of the aortic valves.
- Model III: The aortic valves were irritated for 24 h by the catheter to stimulate pre-damage of the heart valve.



After the stimulus and prior to infection, the catheter was removed during a second surgical intervention.

- Model IV: A ten-second irritation of the aortic valve was performed with a catheter (SHAM group), assuming that no sustained damages (i.e., not anymore present at the time of infection) occurred at the valves. This model was used to assess the burden of surgery and systemic infection without IE formation.

During surgery, the animals were anesthetized with 2% isoflurane and received medication for peri- and postoperative pain (Carprofen; Rimadyl, Pfizer Animal Health, NY, United States). The infectious dose of 10^5 CFU was used, as it was previously shown to reliably induce IE (Ring et al., 2014). On the third day of the experiment (48–56 h after catheter placement), the animals were sacrificed by transcardial perfusion either after the last MRI scan as described below or at defined endpoints (clinical score >20 , see **Supplementary Table S1**). Organs and catheter were harvested for microbiological analysis.

Clinical Score

All animals were scored and examined daily for health status (body weight, body temperature, respiration, physical appearance, behavior, and wound healing from surgical interventions) defined by the approved animal use protocol. Each day, the corresponding score points for each health feature were added up and summarized as clinical score, representing

a quantitative measure of the severity of the disease. Design of the clinical score was based on previous studies (Ring et al., 2014; Shrum et al., 2014) and typical IE symptoms (Kreitmann et al., 2020).

Bacterial Strains

For all infections either the methicillin-susceptible wildtype *S. aureus* strain 6850 (Vann and Proctor, 1987; Fraunholz et al., 2013) or Newman (Duthie and Lorenz, 1952; Baba et al., 2008) was used. Both strains are human isolates. Newman has been used extensively in animal models of staphylococcal disease due to its robust virulence phenotypes (Baba et al., 2008). **Supplementary Figure S1** provides a summary of the different pathogenicity profiles of the two strains, which confirmed previous literature. While for *S. aureus* 6850 strong expression ($p < 0.05$) of cytotoxic and hemolytic toxins such as α -toxin (hla) could be demonstrated (Balwit et al., 1994; Haslinger-Löffler et al., 2005; Haslinger-Löffler et al., 2006; Lam et al., 2010; Strobel et al., 2016) the *S. aureus* strain Newman showed low toxin expression (Dassy et al., 1993; Sause et al., 2017), but pronounced adhesin expression such as staphylococcal protein A (SpA; Hartleib et al., 2000) extracellular adherence protein (Eap; Chavakis et al., 2002; Johnson et al., 2008; Mainiero et al., 2010; Hoen and Duval, 2013) Clumping factor A (ClfA; McDevitt and Foster, 1995; Juuti et al., 2004), and Fibronectin binding protein A (FnBPA), which promote the adherence to

damaged endothelium at the aortic valves. Bacteria were grown in brain heart infusion (BHI) medium overnight, followed by a 3 h culture after a 1:100 dilution of overnight culture in fresh BHI. The bacteria were washed in PBS, adjusted to $OD_{578} = 1$ (optical density at 578 nm) and stored at -80°C until use. Colony forming units were enumerated after serial dilution and overnight growth at 37°C on agar plates. Antibiotic-sensitivity testing was performed on fresh *S. aureus* isolates (Automated VITEK[®] 2 System Version 9.02 (BioMérieux Inc.) (Supplementary Table S2).

Extraction of Bacterial RNA and RT-qPCR

Extraction of bacterial RNA and real-time quantitative polymerase chain reaction (RT-qPCR), including complementary DNA synthesis and real-time amplification was performed as described previously (Tuchscherer et al., 2011). In order to analyze the expression of the virulence factors α toxin (*hla*), staphylococcal protein A (*spa*), extracellular adherence protein (*eap*), Clumping factor A (*clfA*) and Fibronectin binding protein A (*fnbA*), the gene for gyrase B (*gyrB*) was taken as the housekeeping gene. All data were normalized to this gene. Primers used in this study are listed in Table 1.

MR Imaging

Measurements were performed at 9.4T on a BioSpec 94/20 small animal MRI system (Bruker BioSpin, Ettlingen, Germany) equipped with a 1 T/m gradient insert (BGS-6S, Bruker) and ParaVision software version 5.1 (Bruker). A mouse body quadrature volume coil with an inner diameter of 35 mm (Rapid Biomedical, Rimpfing, Germany) was used for image acquisition. During MRI, the mice were anesthetized with isoflurane (1.5–2.5% isoflurane and 0.7/0.3 air/O₂ mixture), and core body temperature and respiration rates were monitored using a MRI compatible monitoring system (SA Instruments, Stony Brook, NY, United States). A self-gated CINE-UTE sequence was used to visualize the infected aortic valves over the cardiac cycle (TR/TE: 5/0.31 ms, FA: 15°, FOV: (3.20 cm²), MTX: 256 × 256, section: 1 mm, scan duration: 12:08 min). 20 images per cardiac cycle were reconstructed retrospectively.

Ex vivo-Analysis

Microbiological Analysis

Spleen, lung, kidney, liver, myocardium, aortic arch, and aortic valves were homogenized, serially diluted in PBS and plated on blood agar plates for bacterial counting. The isolated catheter was first placed in an ultrasound bath for 10 min and then vortexed for 1 min. The catheter supernatant was serially diluted and spread on blood agar plates. All blood agar plates were incubated overnight at 37°C and CFUs were counted subsequently. Corresponding CFUs were determined per mg tissue or catheter, and mean values were plotted in a spider chart. For each chart the area under the curve [AUC, shoelace formula (Braden, 1986)] was calculated, representing the overall bacterial burden of each animal group investigated.

Histology

Serial sections of paraffin-embedded heart valves were prepared with a thickness of 2, 5 or 10 μm for histological analysis. The gram-positive *S. aureus* bacteria were stained with crystal violet/iodine (GRAM) according to standard protocols. Hematoxylin and eosin staining (HE) was used to detect basophilic components (DNA/RNA) and eosinophilic structures (collagen/muscle), and Weigert's Elastica-van-Gieson (EvG) staining was used to label collagen to indicate changes in the blood vessel (Kazlouskaya et al., 2013). Tissue sections were examined under the light microscope (Nikon Eclipse 50i, Nikon-Düsseldorf, Germany) at 60x and 100x primary magnification.

Transmission Electron Microscopy

Aortic valves were removed from each experimental group 24 h post infection and analyzed by transmission electron microscopy (TEM). In brief, heart valves or catheters were fixed in 2% (v/v) formaldehyde and 2.5% (v/v) glutaraldehyde in 100 mM sodium cacodylate buffer, pH 7.4, at 4°C overnight. For heart valves: After washing in PBS, samples were postfixed in 0.5% (v/v) osmium tetroxide and 1% (w/v) potassium hexacyanoferrate III in 100 mM sodium cacodylate buffer for 2 h at 4°C followed by washing with distilled water. After dehydration in an ascending ethanol series from 30 to 100% ethanol, samples were two times incubated in propylenoxide each for 15 min and embedded in Epon (Epoxy Embedding Medium Kit; Sigma, Taufkirchen, Germany) using a flat embedding mold. For catheters: After dehydration in ethanol up to 70%, samples were embedded in LR White medium (London Resin Company, London, United Kingdom), and polymerized using UV light according to the manufactures instructions. Ultrathin sections were cut with an ultramicrotome (Leica Ultracut UCT), collected on copper grids and negatively stained with 2% uranyl acetate for 20 min. Electron micrographs were taken at 60 kV with a Phillips EM-410 electron microscope using imaging plates (Ditabis, Pforzheim, Germany).

Immunohistology

The 2 μm thick sections of the heart valves were dewaxed and boiled in citrate buffer (pH 6) (2 × 2 min). Subsequently, the primary antibody von-Willebrand-factor (vWF) (ab6994; Abcam, United Kingdom; dilution 1:200) was added and incubated overnight at 4°C . Next, unbound primary antibody vWF was removed from the slice and secondary antibody goat-anti-rabbit (Biotin) (B2770 life technologies dilution 1:600) was added to the sections and incubated at room temperature for 1 h. Subsequently the label Alexa Fluor 546 with Streptavidin-Tag (dilution 1:800) was incubated for 45 min at room temperature to bind to the biotin. Finally, DAPI staining, incubating slices for 6 min at room temperature, was used to display the cell nuclei.

Statistical Analysis

Statistical analyzes were performed with the software GraphPad software version 5 (GraphPad Software, La Jolla California United States). For each IE model (I–IV) bacterial titers were analyzed statistically using a one-way ANOVA calculation.

TABLE 1 | Primers used to study bacterial gene expression.

Gene	Primer	Primer-sequence	References
<i>gyrB</i>	Forward	5'-AATTGAAGCAGGCTATGTGT-3'	Tuchscher et al., 2011
	Reverse	5'-ATAGACCATTTTGGTGTGG-3'	
<i>hla</i>	Forward	5'-CAACTGATAAAAAAGTAGGCTGGAAAGTGAT-3'	Tuchscher et al., 2011
	Reverse	5'-CTGGTGAAAACCCTGAAGATAATAGAG-3'	
<i>clfA</i>	Forward	5'-GAATCAGCTCCACAGAGTACAG-3'	Kalinka et al., 2014
	Reverse	5'-TCTCATTCTAGGCGCACTTG-3'	
<i>eap</i>	Forward	5'-AGTCATTGATTACAACAA-3'	Joost et al., 2009; Kalinka et al., 2014
	Reverse	5'-CTTATTAATGTAAAGCTTG-3'	
<i>fnbA</i>	Forward	5'-ACAAGTTGAAGTGGCACAGCC-3'	Tuchscher et al., 2011
	Reverse	5'-CCGCTACATCTGCTGATCTTGTC-3'	
<i>spa</i>	Forward	5'-CAGATAACAATTAGCTGATAAAAAACAT-3'	Roberts et al., 2006; Kalinka et al., 2014
	Reverse	5'-CTAAGGCTAATGATAATCCACCAAATAC-3'	

Bacterial load on the valves was compared to that in all other organs after Bonferroni correction. A value of $p < 0.05$ was considered as significant.

Ethics Statement

All animal experiments were approved by the North Rhine-Westphalia Agency for Nature, Environment, and Consumer Protection (Landesamt für Natur, Umwelt und Verbraucherschutz Nordrhein-Westfalen-LANUV; ID 87-51.04.2011.A003; ID 84-02.04.2015.A581).

RESULTS

Magnetic Resonance Imaging

Four mouse models of IE with different surgical interventions (I–IV, **Figure 1**), were infected with the *S. aureus* strain 6850 or Newman and were examined with respect to abnormal valve formations by *in vivo* MRI (see **Supplementary Movies S1–S12**). Only the IE model I demonstrated thickened heart valves after inoculation with either *S. aureus* strain (**Figure 2**; also see **Supplementary Movies S2, S3**). Especially *S. aureus* 6850-infected valves presented additional structures such as for example pendulum-like masses. On these valves the presence of pronounced vegetations could be confirmed by macroscopic examination after the organ had been harvested. Black-brown deposits could further be identified on the valves of perfused hearts due to the aggregation of thrombocytes (see **Figures 2d,j,p,v**) during the infection (Liesenborghs et al., 2019). The other three modified models of IE (II–IV) showed fragile and healthy valve structures similar to those of the MOCK groups having received a PBS injection.

Histology

To examine morphological conspicuities of the heart valves such as thickening and additional structures in IE model I, histological analysis was performed on valve sections using GRAM, HE and Weigert's EvG staining. In naïve control animals, no evidence of inflammation was found in either staining. In contrast, animals with *S. aureus* infection and irritated aortic

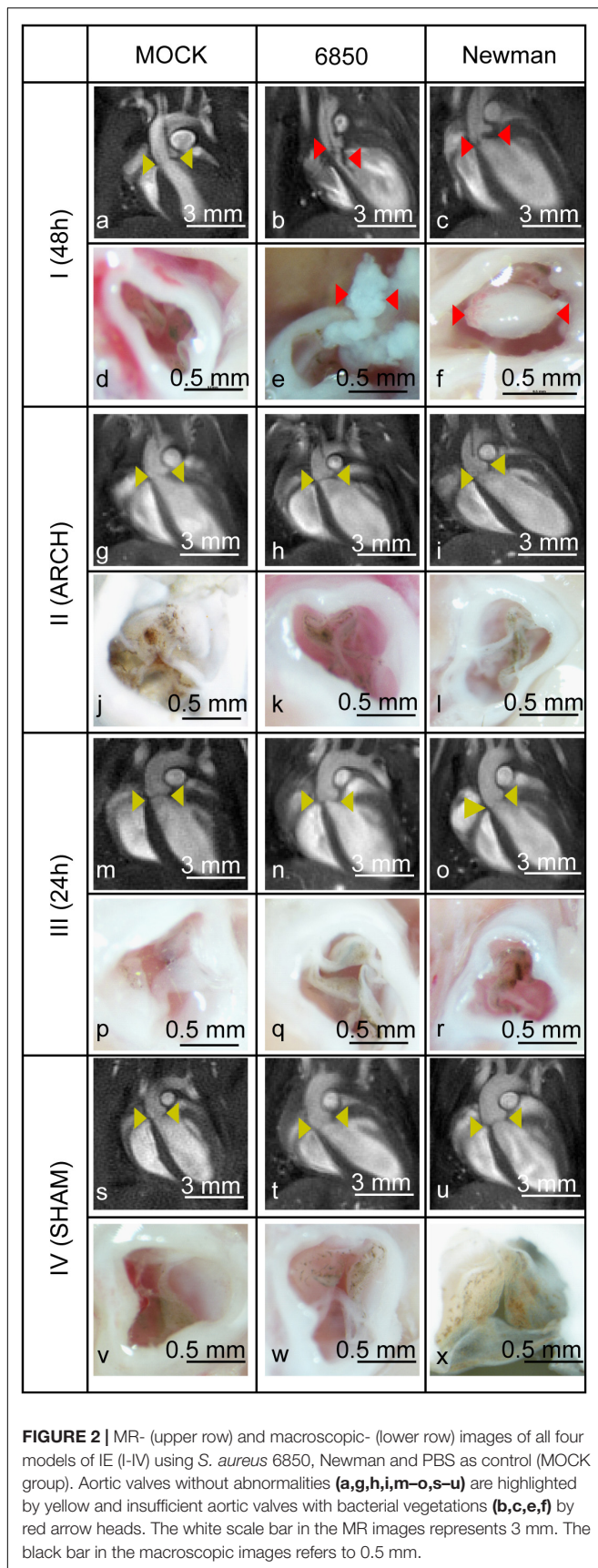
valves, clearly revealed bacterial vegetations on the aortic valves and also partly in the adjacent soft tissue. The bacteria formed extended clusters on the valves resulting in occasionally solid amorphous structures (**Figure 3**, red arrows). These structures could not be identified as collagen in Weigert's EvG staining (blue arrows). Especially at the root of the valve and at the adjacent tissue a fulminant infiltration and accumulation of immune cells, i.e., mainly neutrophilic granulocytes (HE staining, black arrows) were observed with both *S. aureus* strains. Unambiguous strain-specific morphological manifestations in the valvular cellular structures during IE could not be identified.

Colony Forming Unit

To assess the extent of localized *S. aureus* vegetations on the aortic valves, bacterial distributions of either *S. aureus* strain (Newman or 6850) were investigated in all four models of IE (I–IV) 24 h post infection by counting CFUs (**Figure 4**). For both strains, the aortic valves of model I revealed an average bacterial load of 10^9 CFU / mg tissue and thus differed significantly from the results in spleen, lung, liver, and kidney (**Figures 4A,B**). Infections with the strain 6850 showed similar bacterial load (AUC = 9.6 ± 1.1 , **Figure 4I**) compared to Newman infections (AUC = 9.2 ± 2.0 , **Figure 4J**).

In contrast, in model II, having the catheter placed in the aortic arch instead of the aortic root, the highest bacterial load (6850: 10^8 CFU/mg tissue, Newman: 10^6 CFU/mg tissue) was counted in the aortic arch. Local infection was higher than on the aortic valves (6850: 10^6 CFU/mg tissue, Newman: 10^4 CFU / mg tissue), representing a significant difference in bacteria counts in Newman infections (**Figures 4C,D**). Altogether, in model II, Newman infections (AUC = 8.4 ± 1.7 , **Figure 4J**) resulted in a greater overall bacterial burden in comparison to infections induced with *S. aureus* 6850 (AUC = 7.8 ± 1.0 , **Figure 4I**). Macroscopic and microscopic analysis of the catheter revealed adherent bacteria and bacterial vegetations on the catheter tip, providing a permanent source of infection (**Figure 5**).

In model III, an irritation was performed by the catheter on the aortic valves for 24 h only. In infections with strain 6850, a high bacterial load of 4×10^8 CFU/mg tissue was counted on the heart valves. Bacterial burden was similar in all organs



investigated (**Figure 4E**). In contrast, for Newman infections only low levels of CFU values were counted on the aortic valves as well as in all other organs (up to 10^3 CFU/mg tissue, **Figure 4F**). Infections with *S. aureus* 6850 (AUC = 8.6 ± 2.5 , **Figure 4I**) resulted in approximately twice as high over all bacterial burdens as compared to infections with *S. aureus* Newman (AUC = 4.7 ± 1.4 , **Figure 4J**).

In model IV, the shortest irritation time of the aortic valve was used among all four models. Inoculation with either *S. aureus* 6850 or Newman resulted in the overall lowest bacterial burden compared to the other three IE models (I–III). Lung and spleen showed the strongest infection (6850: 10^4 CFU/mg tissue; Newman: 10^3 CFU/mg, **Figures 4G,H**) and no bacteria were found on the heart valves. In general, in model IV infections with *S. aureus* 6850 (AUC = 5.5 ± 2.1 , **Figure 4I**) led to a higher bacterial load than infections with *S. aureus* Newman (AUC = 4.0 ± 1.2 , **Figure 4J**).

To further assess the underlying degree of endothelial damage, immunohistological investigations were performed in all four models of IE, 24 h post mock infection, by qualitative analysis of vWF expression (Goncharov et al., 2017) on the aortic valves. Those revealed pronounced vWF expression (red) in model I and minor vWF expression in model III (**Figure 6**). No vWF expression was detected in models II and IV as well as in healthy naïve animals.

Altogether, our results showed that model I involving both endothelial damage as well as a continuous bacterial source such as adherent bacteria on the catheter, lead to the most pronounced manifestation of IE.

Clinical Score

All four mouse models of IE were evaluated with regards to their clinical scores, which were then correlated to the corresponding bacterial burden. The MOCK groups of all four different models of IE (I–IV) that did not receive any pathogen infection showed mild to moderate clinical scores in the range of 4–12 (**Figure 7**). In Newman infections, almost the same clinical scores were observed in the corresponding models of IE, even though higher overall bacterial counts with AUC values up to levels of 10^9 CFU/mg tissue and 10^8 CFU/mg tissue were observed in model I and II, respectively. In contrast, inoculation of mice with *S. aureus* 6850 resulted in high clinical scores of 23 ± 3.0 and 26 ± 5.4 in IE model I and II, respectively, while similar bacterial burdens of 10^9 CFU/mg tissue and 10^8 CFU/mg tissue were observed, respectively. These animals clearly showed severe symptoms of sepsis such as weight loss, lethargy, as well as a high bacterial load in all organs studied. Model III and IV showed only mild symptoms of infection and also revealed the lowest bacterial counts in spleen, lung, liver, and kidney. These models were scored with similar clinical findings as the corresponding MOCK groups. Taken together, our results reveal a discrepancy between number of bacteria on the valves and clinical symptoms. While the extent of local vegetations on the heart valves mainly depended on degree of tissue injury and presence of bacteria in the blood stream, the clinical picture was dominated by pathogenicity and virulence factor profile of the respective *S. aureus* strain.

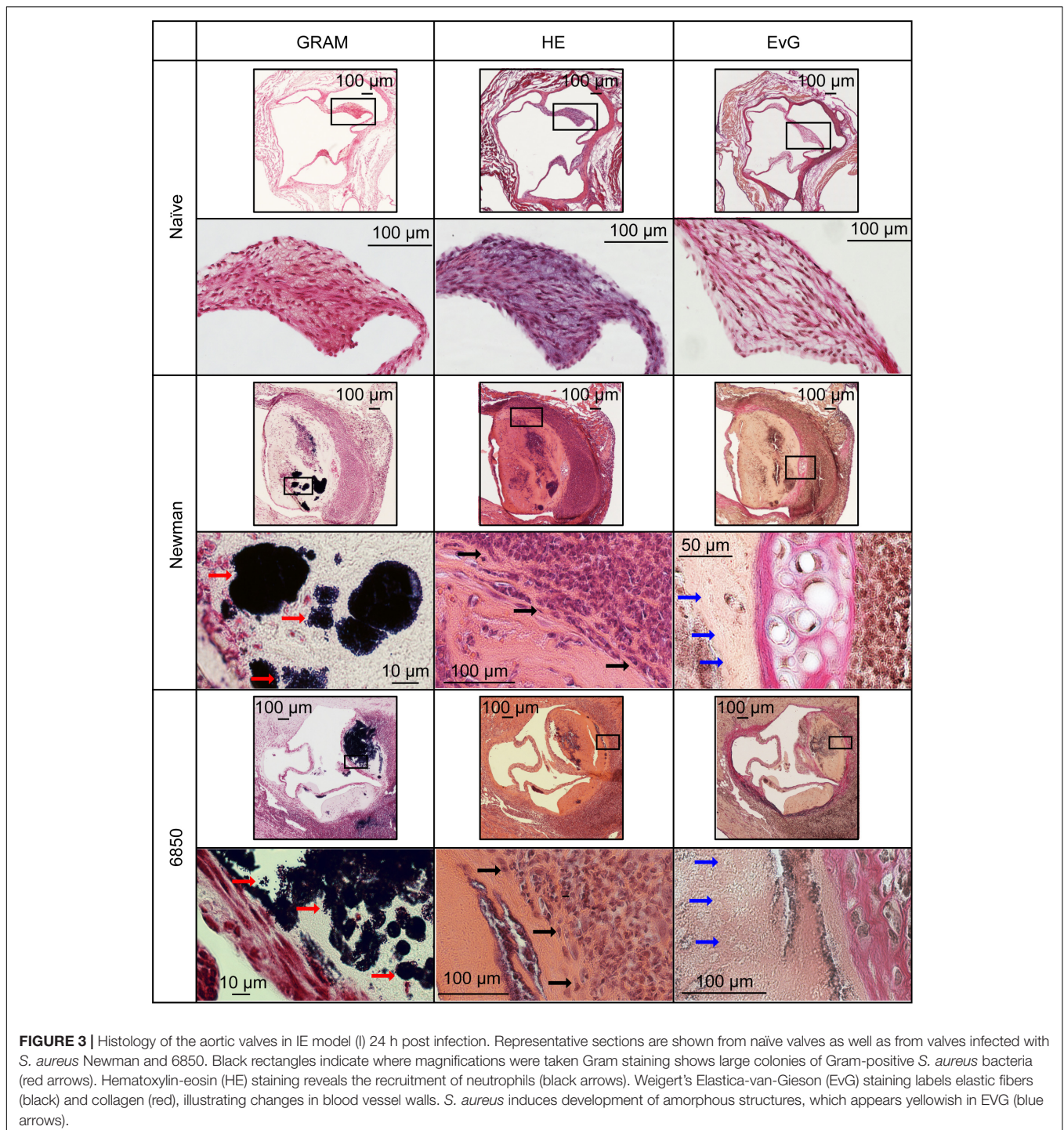


FIGURE 3 | Histology of the aortic valves in IE model (I) 24 h post infection. Representative sections are shown from naïve valves as well as from valves infected with *S. aureus* Newman and 6850. Black rectangles indicate where magnifications were taken. Gram staining shows large colonies of Gram-positive *S. aureus* bacteria (red arrows). Hematoxylin-eosin (HE) staining reveals the recruitment of neutrophils (black arrows). Weigert's Elastica-van-Gieson (EvG) staining labels elastic fibers (black) and collagen (red), illustrating changes in blood vessel walls. *S. aureus* induces development of amorphous structures, which appears yellowish in EVG (blue arrows).

DISCUSSION

In this study, the differential impact of host and pathogen factors on severity of IE was investigated by imaging and microbial analysis of four different surgical IE models, each infected with two different *S. aureus* strains. Several animal models have been established over the last years (Highman et al., 1959; Garrison and Freedman, 1970; Durack and Beeson, 1972; Durack et al.,

1973; Baddour et al., 1984; Sande and Zak, 1999; Gibson et al., 2007; Veloso et al., 2011) to advance the understanding of the underlying pathogenesis of IE and to improve current diagnostic and therapeutic interventions. All animal models of IE share comparable procedures, beginning with valve trauma through mechanical irritation by placing a catheter on the aortic root, followed by intravenous infection with a bacterial dose between 10^5 and 10^8 CFUs (Gibson et al., 2007; Ring et al., 2014;

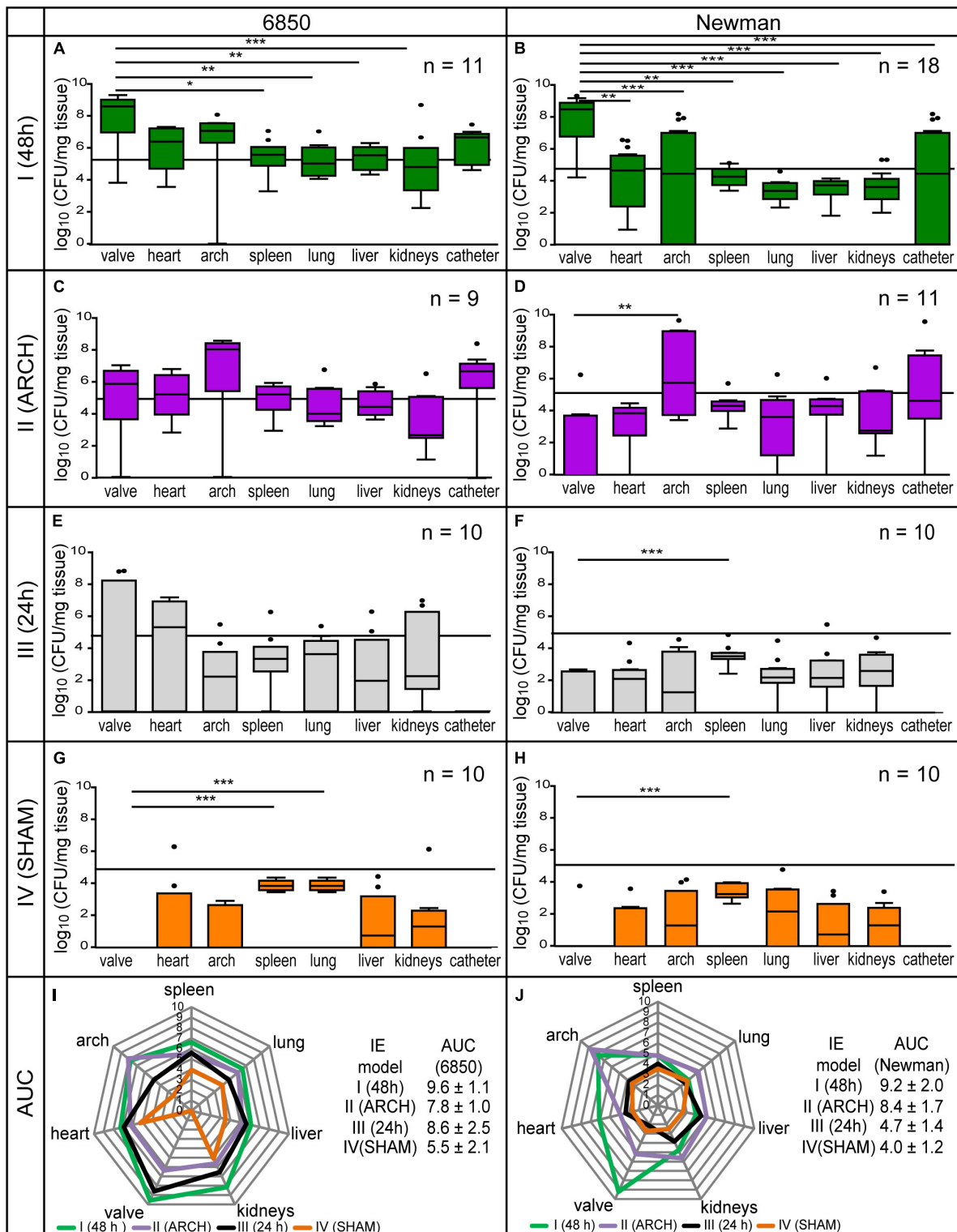
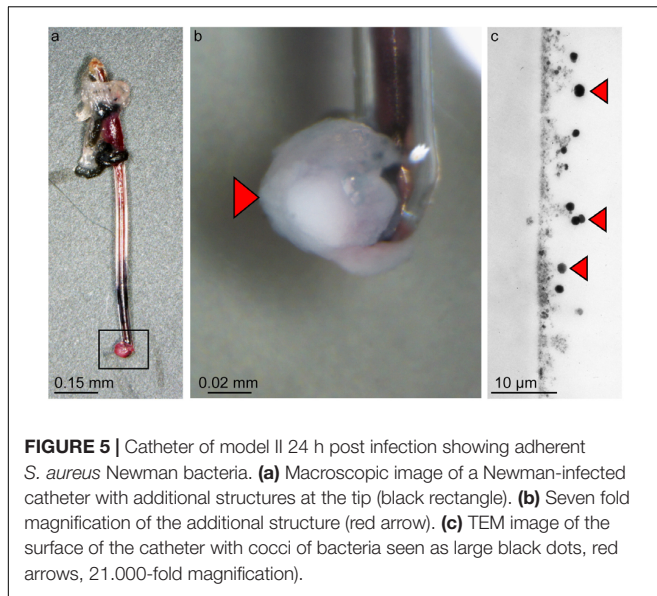


FIGURE 4 | Microbial analysis of four different models of IE (I–IV) using the *S. aureus* strains 6850 and Newman. **(A,B)** Shows model I, **(C,D)** shows model II, **(E,F)** shows model III, **(G,H)** shows model IV. The bacterial injection dose of 10^5 CFU is marked as a black threshold in the respective graphs of the corresponding bacterial counts in different organs. The results are displayed as box and whiskers plots, with data between first and third quartiles, the band in the box stands for the second quartile (=median). Whiskers represent lowest and highest data within 1.5 interquartile ranges of the lower and upper quartile. The overall bacterial load is shown as spider web chart for all four models of IE induced with *S. aureus* 6850 **(I)** and Newman **(J)**, 24 h post infection. For each model the corresponding bacterial burden is calculated as area under the curve (AUC). * $p < 0.05$, ** $p < 0.01$, *** $p < 0.001$.



Liesenborghs et al., 2019). In many models the catheter remains in place during the induction of infection and possibly has a high impact on disease progression due to adherent bacteria on the catheter forming a permanent source of infection (Baddour et al., 1984; Sande and Zak, 1999; Ring et al., 2014). In our study, we systematically investigated the influence of the catheter and endothelial damage on formation of bacterial vegetations on the aortic valves and overall bacterial distribution. To this end, in the models we either placed the catheter at the aortic root for 48 h (I), 24 h (III) or 10 s (IV, SHAM) or at the aortic arch for 48 h (II) and infected the animals with *S. aureus* 6850 or Newman 24 h post-surgery.

Damage

In consideration of the different bacterial burdens found on the aortic valves in all four models of IE, our results demonstrate that the endothelial damage is one of the key factors in the induction of IE. Only in model I, having a catheter placed at the aortic root for 48 h, pronounced vegetations of *S. aureus* 6850 and Newman could be detected on the valves in MR and macroscopic images. Histology and CFU counts confirmed the presence of large amounts of bacterial colonies in the range of 10^9 CFU/mg tissue as well as immune cell infiltration. Compared to the models II-IV, the irritation of the aortic valves for 48 h in model I induced severe endothelial activation and injury resulting in strong release of vWF (Sadler, 1998; Starke et al., 2011; Goncharov et al., 2017; Mehta et al., 2019; **Figure 6**). In model III only mild vWF-expression was detected, while in model IV the irritation of the aortic valves for 10 sec did not result in detectable vWF expression. Severe damage seems to promote strong bacterial adhesion (Liesenborghs et al., 2019). It is well known that vWF, an adhesive glycoprotein which is located in the subendothelial layers of the blood vessel wall, such as the intima layer (Sadler, 1998; De Meyer et al., 2009) is one of the key binding factors during the formation of *S. aureus* IE

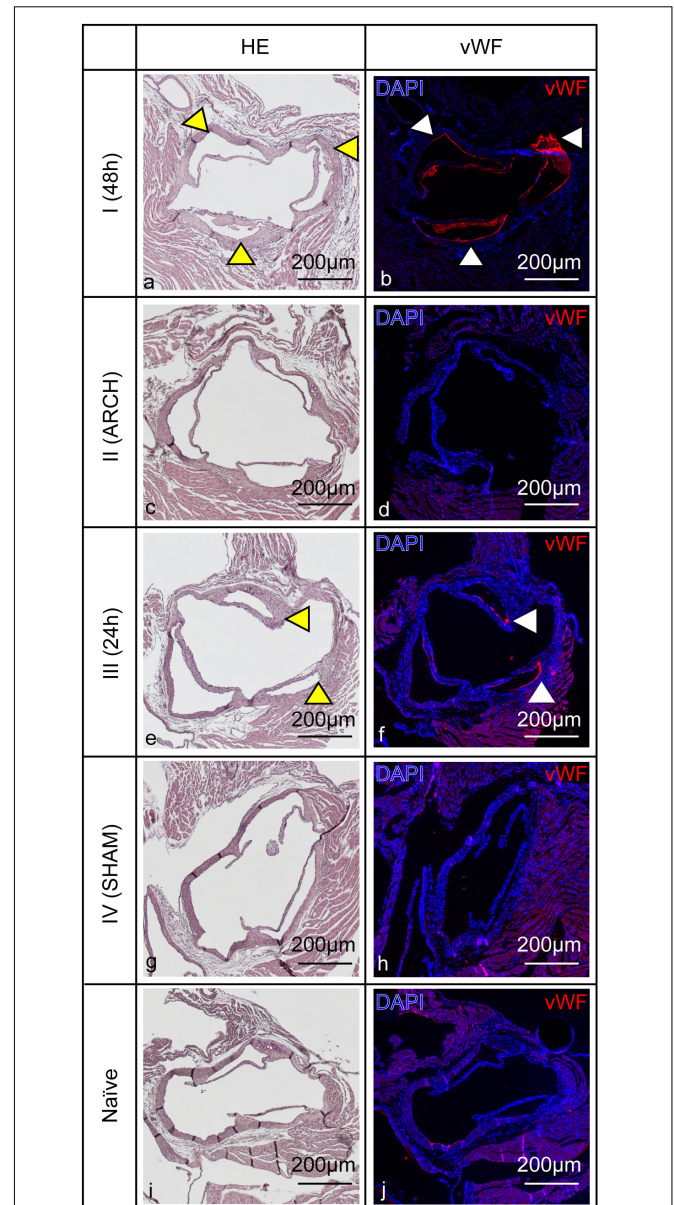
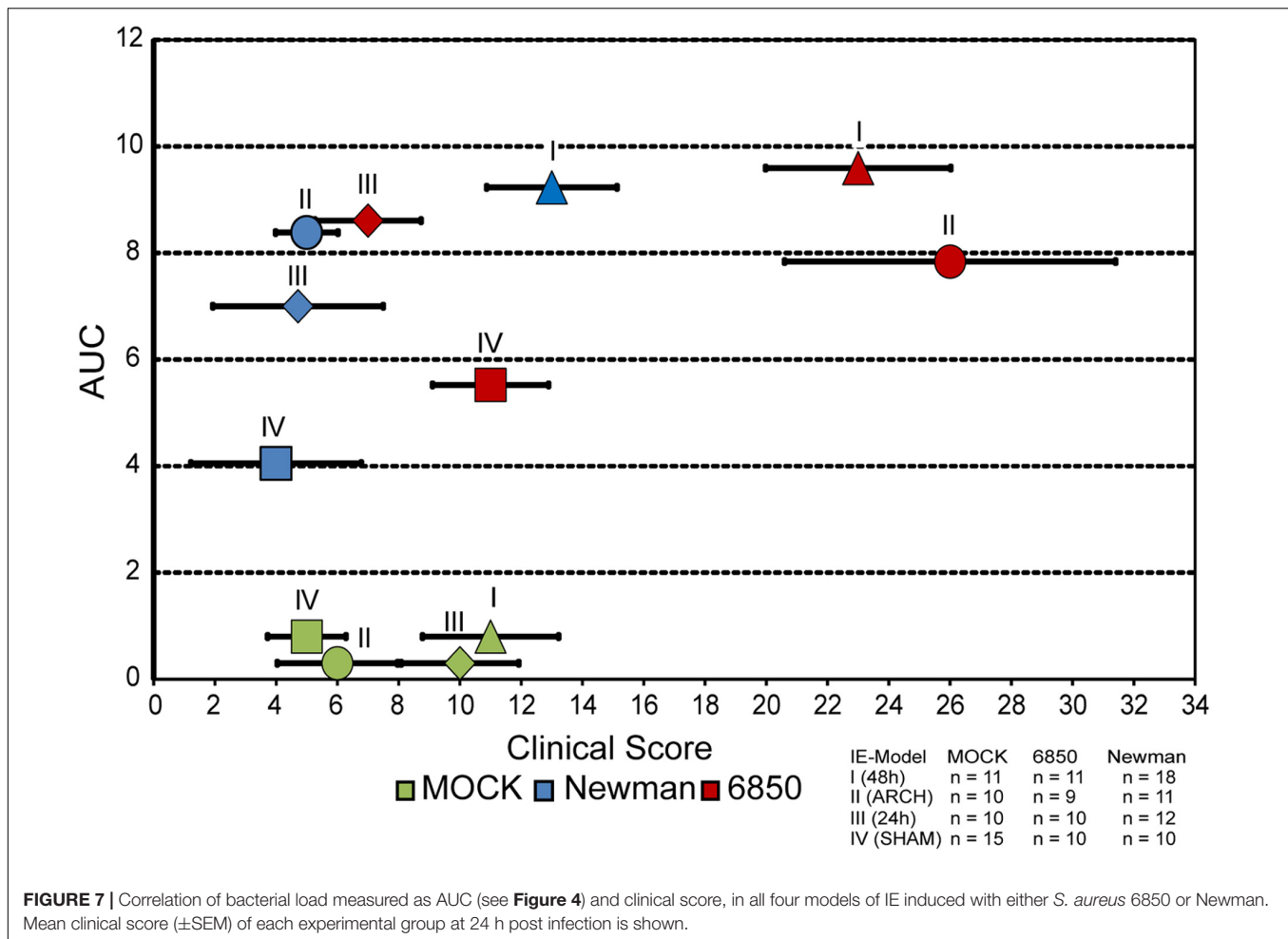


FIGURE 6 | Endothelial damage of the aortic valves induced by corresponding catheter placement in all four models of IE (I-IV) with MOCK-infection. **(a,c,e,g,i)** Hematoxylin-eosin staining shows anatomical cellular structures of the aortic valves. **(b,d,f,h,j)** Cell nuclei are visualized by DAPI fluorescence staining, immunohistological staining identifies vWF expression especially in model I **(b)** and III **(f)** (red signal, white arrow heads). Hematoxylin-eosin staining shows anatomical cellular structures of the aortic valves (left column). Cell nuclei are visualized by DAPI fluorescence staining (blue signal in the right column). Immunohistological staining identifies vWF expression especially in model I and III (red, white arrow heads). Corresponding anatomical structures are pointed out with yellow and white arrow heads. Scale bars indicate 200 μm.

(Pappelbaum et al., 2013; Claes et al., 2017; Liesenborghs et al., 2018). At sites of endothelial damage and injury, vWF presents on the vascular surface and promotes the adherence of *S. aureus* through its virulence complexes of Clumping factor A (ClfA;



Claes et al., 2017) and von Willebrand factor-binding protein (vWbp; Bjerketorp et al., 2004). Both *S. aureus* 6850 and Newman showed comparable numbers of bacteria on the valves.

Bacteremia

In addition to the strong endothelial damage induced by the catheter in model I, the catheter represented also a permanent source of infection. Besides an intensive inoculation of the heart valves, other organs such as liver, kidney, spleen, lung, heart, and aortic arch also showed high bacterial counts, indicating an unspecific systemic bacterial infection, possibly caused by the bacterial adherence on the catheter (von Eiff et al., 1999; Höök and Foster, 2000; Maira-Litrán et al., 2002; O'Grady et al., 2002; Pant et al., 2018). Model II containing the catheter at the aortic arch without damaging the endothelial layers of the aortic valves also resulted in an overall high number of bacterial counts in different organs. Both with (model I) and without (model II) endothelial damage, the bacterial infection resulted in a similar overall bacterial manifestation and burden, with a high number of bacteria on the aortic valves. These results suggest that the presence of a permanent bacterial source is decisive for the formation of IE. Comparison of model II–IV and I–III support these findings. The presence of the catheter with or without

underlying endothelial damage leads to an almost two fold higher overall bacterial burden (AUC values). In previous studies it was shown that the presence of a catheter during the infection enhanced the infective dose (Zimmerli et al., 1982).

Clinical Picture

Our results suggest that the overall bacterial distribution and the amount of substantially infected organs, rather than the bacterial load on the aortic valve, influence the clinical picture (Singer et al., 2016; Xie et al., 2017). The highest disease severity was found in model I and II with 6850 infections, while all other infection models showed only moderate infection symptoms, similar to animals with MOCK infections (**Supplementary Figure S2**).

Adhesion

Even though both in model I and II similar bacterial concentrations were found at the aortic valves for *S. aureus* 6850 and Newman, both the clinical picture and manifestations of the corresponding bacterial vegetation differed substantially on macroscopic levels. *S. aureus* IE induced by the bacterial strain 6850 led to fulminant additional structures on the valves composed of *S. aureus* bacteria, immune cells and connective

tissue (**Figure 3**), in agreement with previous studies (Kolar and Liu, 2016). These structures presented along with severe tissue damage and destruction. In contrast, *S. aureus* Newman infections generally occurred in form of valve thickening. Even though, histologically, no substantial differences in the tissue morphology could be found, possible reasons for these macroscopic observations might be found in the bacteria-specific adhesin and toxin profiles and thus differences in pathogenicity. Both *S. aureus* 6850 and Newman produce fibronectin binding proteins (FnBPs; **Supplementary Figure S1**). However, in *S. aureus* Newman, despite high expression levels, they are not anchored to the cell wall, which leads to a loss of FnBP-dependent functions (Haslinger-Löffler et al., 2005). In contrast *S. aureus* 6850 expresses low levels of this adhesin on the cellular surface, which mediates efficient adherence to activated and injured tissue (Vann and Proctor, 1987; Balwit et al., 1994; Haslinger-Löffler et al., 2005; Haslinger-Löffler et al., 2006; Lam et al., 2010; Seidl et al., 2011; Seidl and Zinkernagel, 2013; Strobel et al., 2016). In 6850, high expression levels of hemolytic peptides such as α - (Berube and Wardenburg, 2013; Surewaard et al., 2018), β -, γ - and δ - toxins were previously described and verified, which can cause necrotic death of the target host cell and thus induce severe tissue destruction (Vandenesch et al., 2012). There is increasing evidence that the strain is also able to escape from phagolysosomes in immune cells such as macrophages, neutrophils and dendritic cells. Through the expression of phenol-soluble modulins and β -toxin (Strobel et al., 2016) the bacteria strain is less vulnerable to the host response system and promotes cell destruction (Giese et al., 2011; Grosz et al., 2014). Even though different adhesin profiles are discussed and observed for 6850 (Balwit et al., 1994) and Newman (Novick, 2003; Traber et al., 2008; **Supplementary Figure S1**), equal bacterial counts were observed on the catheter for both strains in models I and II (**Figures 4A–D**). However, in both models *S. aureus* 6850 induced more severe infections of other organs such as lung, liver spleen and kidney, and resulted in higher clinical scores. The aggressive character of the *S. aureus* 6850 became also obvious when comparing the ability of the two *S. aureus* strains to induce IE in model III. The short irritation of the aortic valves for 24 h resulted in decreased vWF release as evidenced by immunohistological analysis. Yet, high bacterial counts on the aortic valves and the heart were observed for infections with 6850, but not for infections induced by *S. aureus* Newman. In contrast to models I and II, in absence of a persisting catheter even *S. aureus* 6850 induced only a moderate bacterial load in the other organs such as liver, spleen, lung and kidney. At the same time, these animals showed milder disease symptoms and reached clinical score values between 4 and 8, which were comparable to those of MOCK infected animals.

CONCLUSION

In conclusion, the four different modifications of IE animal models, investigated in our study using two different *S. aureus* strains, take major steps of the pathogenesis of *S. aureus* IE into account – bacterial adhesion at the site of endothelial

damage, constant bacteremia and cellular and inflammatory response. Our results showed, that independent of the bacterial strain, pronounced bacterial vegetations on the valves were only formed when the two key factors of endothelial damage and continuous bacterial source were present simultaneously. To induce sufficient endothelial damage, an irritation of the aortic valves by the catheter for at least 24 h was necessary. The longer the catheter remained in place at the aortic valve, the greater the endothelial damage. However, severe endothelial damage in the absence of a permanent bacterial source resulted in reduced valve infection and was strongly dependent on the pathogenic profile of the infectious agent. In contrast, the presence of a foreign body and thus a permanent bacterial source alone caused unspecific overall high bacterial loads and distributions in major organs such as kidney, liver, spleen, lung and heart. The amount of bacteria strongly differed between bacterial strains, which might be regulated by the bacteria-specific affinity to tissue and the catheter. These findings underline that the endothelial activation and injury is the major cause to trigger and promote the formation of IE. The catheter itself additionally fosters the bacterial distribution in other organs and overall systemic infection and its severity.

DATA AVAILABILITY STATEMENT

All datasets generated for this study are included in the article/**Supplementary Material**.

ETHICS STATEMENT

The animal study was reviewed and approved by Landesamt für Natur, Umwelt und Verbraucherschutz Nordrhein-Westfalen-LANUV.

AUTHOR CONTRIBUTIONS

CF, CS, and VHoe designed the study. AJ (histology), CS (animal models, histology, microbiology, MRI), HV (microbiology), SN (PCR), UH (TEM), VHös (histology, microbiology), VHoe (histology, MRI), and YT (animal models) performed experiments. AJ (histology), CS (animal models, histology, microbiology, MRI), HV (microbiology), MK (histology), SN (PCR, microbiology), UH (TEM), VHös (histology, microbiology), and VHoe (histology, MRI) analyzed data. CF, CS, MW, and VHoe wrote the manuscript. All authors interpreted data, and revised, and edited the manuscript.

FUNDING

This work was supported by the German Research Foundation, SFBTR34-C14, and the Interdisciplinary centre for clinical research (IZKF) Muenster, IZKF-Fa2/014/18 and IZKF-PIX.

ACKNOWLEDGMENTS

We thank Karin Schlattmann and Brigitte Schuhen for excellent technical assistance.

SUPPLEMENTARY MATERIAL

The Supplementary Material for this article can be found online at: <https://www.frontiersin.org/articles/10.3389/fmicb.2020.01325/full#supplementary-material>

FIGURE S1 | Gene-expression of the α toxin (hla) and different adhesion molecules such as staphylococcal protein A (spA), extracellular adherence protein (eap), Clumping factor A (clfA) and Fibronectin binding protein A (fnbA) in *S. aureus* 6850 (white boxes) and Newman (gray boxes). The results ($n = 6$ out of three independent cultures) are displayed as box and whiskers plots, with data between first and third quartiles, the band in the box stands for the second quartile (=median). Whiskers represent lowest and highest data within 1.5 interquartile ranges of the lower and upper quartile. * $p < 0.05$, ** $p < 0.01$.

FIGURE S2 | Correlation of number of infected organs and clinical score, in all four models of IE induced with either *S. aureus* 6850 or Newman. Mean clinical score (\pm SEM) of each experimental group at 24 h post infection and the corresponding number of infected organs ($\geq 10^5$ CFU / mg tissue, see **Figure 4**) is shown.

TABLE S1 | Clinical Score.

TABLE S2 | Antibiotype of *Staphylococcus aureus* strains 6850 and Newman.

REFERENCES

- Angrist, A. A. (1963). Pathogenesis of Bacterial Endocarditis. *JAMA* 183, 249–252.
- Baba, T., Bae, T., Schneewind, O., Takeuchi, F., and Hiramatsu, K. (2008). Genome sequence of *Staphylococcus aureus* strain Newman and comparative analysis of staphylococcal genomes: polymorphism and evolution of two major pathogenicity islands. *J. Bacteriol.* 190, 300–310. doi: 10.1128/jb.01000-07
- Baddour, L. M., Christensen, G. D., Hester, M. G., and Bisno, A. L. (1984). Production of experimental endocarditis by coagulase-negative Staphylococci: variability in species virulence. *J. Infect. Dis.* 150, 721–727. doi: 10.1093/infdis/150.5.721
- Baddour, L. M., Wilson, W. R., Bayer, A. S., Fowler, V. G., Bolger, A. F., Levison, M. E., et al. (2005). Infective endocarditis: diagnosis, antimicrobial therapy, and management of complications: a statement for healthcare professionals from the Committee on Rheumatic Fever, Endocarditis, and Kawasaki Disease, Council on Cardiovascular Disease in the Young, and the Councils on Clinical Cardiology, Stroke, and Cardiovascular Surgery and Anesthesia, American Heart Association: endorsed by the Infectious Diseases Society of America. *Circulation* 111, e394–e434.
- Balwit, J. M., Langevelde, P. V., Vann, J. M., and Proctor, R. A. (1994). Gentamicin-resistant menadione and hemin auxotrophic *Staphylococcus aureus* persist within cultured endothelial cells. *J. Infect. Dis.* 170, 1033–1037. doi: 10.1093/infdis/170.4.1033
- Bancsi, M. J., Veltrop, M. H., Bertina, R. M., and Thompson, J. (1996). Role of phagocytosis in activation of the coagulation system in *Streptococcus sanguis* endocarditis. *Infect. Immun.* 64, 5166–5170. doi: 10.1128/iai.64.12.5166-5170.1996
- Berube, B., and Wardenburg, J. (2013). *Staphylococcus aureus* α -toxin: nearly a century of intrigue. *Toxins* 5, 1140–1166. doi: 10.3390/toxins5061140
- Bjerketorp, J., Jacobsson, K., and Frykberg, L. (2004). The von Willebrand factor-binding protein (vWbp) of *Staphylococcus aureus* is a coagulase. *FEMS Microbiol. Lett.* 234, 309–314. doi: 10.1111/j.1574-6968.2004.tb09549.x
- Braden, B. (1986). The surveyor's area formula. *College Math. J.* 17, 326–337.
- Bussani, R., De-Giorgio, F., Pesel, G., Zandonà, L., Sinagra, G., Grassi, S., et al. (2019). Overview and comparison of infectious endocarditis and non-infectious endocarditis: a review of 814 autopsic cases. *In Vivo* 33, 1565–1572. doi: 10.21873/invivo.11638
- Chavakis, T., Hussain, M., Kanse, S. M., Peters, G., Bretzel, R. G., Flock, J. I., et al. (2002). *Staphylococcus aureus* extracellular adherence protein serves as anti-inflammatory factor by inhibiting the recruitment of host leukocytes. *Nat. Med.* 8, 687–693. doi: 10.1038/nm728
- Claes, J., Liesenborghs, L., Peetermans, M., Veloso, T. R., Missiakas, D., Schneewind, O., et al. (2017). Clumping factor A, von Willebrand factor-binding protein and von Willebrand factor anchor *Staphylococcus aureus* to the vessel wall. *J. Thromb. Haemost.* 15, 1009–1019. doi: 10.1111/jth.13653
- Dassy, B., Hogan, T., Foster, T. J., and Fournier, J. M. (1993). Involvement of the accessory gene regulator (agr) in expression of type 5 capsular polysaccharide by *Staphylococcus aureus*. *J. Gen. Microbiol.* 139(Pt 6), 1301–1306. doi: 10.1099/00221287-139-6-1301
- De Meyer, S. F., Deckmyn, H., and Vanhoorelbeke, K. (2009). von Willebrand factor to the rescue. *Blood* 113, 5049–5057. doi: 10.1182/blood-2008-10-165621
- Durack, D. T., and Beeson, P. B. (1972). Experimental bacterial endocarditis. I. Colonization of a sterile vegetation. *Br. J. Exp. Pathol.* 53, 44–49.
- Durack, D. T., Beeson, P. B., and Petersdorf, R. G. (1973). Experimental bacterial endocarditis. 3. Production and progress of the disease in rabbits. *Br. J. Exp. Pathol.* 54, 142–151.
- Duthie, E. S., and Lorenz, L. L. (1952). Staphylococcal coagulase; mode of action and antigenicity. *J. Gen. Microbiol.* 6, 95–107.
- Else, R. W., and Holmes, J. R. (1972). Cardiac pathology in the horse. 1. Gross pathology. *Equine Vet. J.* 4, 1–8. doi: 10.1111/j.2042-3306.1972.tb03868.x
- Fraunholz, M., Bernhardt, J., Schuldes, J., Daniel, R., Hecker, M., and Sinha, B. (2013). Complete genome sequence of *Staphylococcus aureus* 6850, a highly cytotoxic and clinically virulent methicillin-sensitive strain with distant relatedness to prototype strains. *Genome Announc.* 1:e00775-13.
- Garrison, P. K., and Freedman, L. R. (1970). Experimental endocarditis I. Staphylococcal endocarditis in rabbits resulting from placement of a polyethylene catheter in the right side of the heart. *Yale J. Biol. Med.* 42, 394–410.
- Gibson, G. W., Kreuser, S. C., Riley, J. M., Rosebury-Smith, W. S., Courtney, C. L., Juneau, P. L., et al. (2007). Development of a mouse model

- of induced *Staphylococcus aureus* infective endocarditis. *Comp. Med.* 57, 563–569.
- Giese, B., Glowinski, F., Paprotka, K., Dittmann, S., Steiner, T., Sinha, B., et al. (2011). Expression of delta-toxin by *Staphylococcus aureus* mediates escape from phago-endosomes of human epithelial and endothelial cells in the presence of beta-toxin. *Cell. Microbiol.* 13, 316–329. doi: 10.1111/j.1462-5822.2010.01538.x
- Goncharov, N. V., Nadeev, A. D., Jenkins, R. O., and Avdonin, P. V. (2017). Markers and biomarkers of endothelium: when something is rotten in the state. *Oxid. Med. Cell. Longev.* 2017:9759735.
- Grosz, M., Kolter, J., Paprotka, K., Winkler, A.-C., Schäfer, D., Chatterjee, S. S., et al. (2014). Cytoplasmic replication of *Staphylococcus aureus* upon phagosomal escape triggered by phenol-soluble modulins α . *Cell. Microbiol.* 16, 451–465. doi: 10.1111/cmi.12233
- Gupta, R. K., Alba, J., Xiong, Y. Q., Bayer, A. S., and Lee, C. Y. (2013). MgrA activates expression of capsule genes, but not the α -toxin gene in experimental *Staphylococcus aureus* endocarditis. *J. Infect. Dis.* 208, 1841–1848. doi: 10.1093/infdis/jit367
- Habib, G., Lancellotti, P., Antunes, M. J., Bongiorno, M. G., Casalta, J.-P., Del Zotti, F., et al. (2015). 2015 ESC Guidelines for the management of infective endocarditis: the task force for the management of infective endocarditis of the European Society of Cardiology (ESC). Endorsed by: European Association for Cardio-Thoracic Surgery (EACTS), the European Association of Nuclear Medicine (EANM). *Eur. Heart J.* 36, 3075–3128. doi: 10.1093/eurheartj/ehv319
- Hartleib, J., Köhler, N., Dickinson, R. B., Chhatwal, G. S., Sixma, J. J., Hartford, O. M., et al. (2000). Protein A is the von Willebrand factor binding protein on *Staphylococcus aureus*. *Blood* 96, 2149–2156.
- Haslinger-Löffler, B., Kahl, B. C., Grundmeier, M., Strangfeld, K., Wagner, B., Fischer, U., et al. (2005). Multiple virulence factors are required for *Staphylococcus aureus*-induced apoptosis in endothelial cells. *Cell. Microbiol.* 7, 1087–1097. doi: 10.1111/j.1462-5822.2005.00533.x
- Haslinger-Löffler, B., Wagner, B., Bruck, M., Strangfeld, K., Grundmeier, M., Fischer, U., et al. (2006). *Staphylococcus aureus* induces caspase-independent cell death in human peritoneal mesothelial cells. *Kidney Int.* 70, 1089–1098. doi: 10.1038/sj.ki.5001710
- Héraïef, E., Glauser, M. P., and Freedman, L. R. (1982). Natural history of aortic valve endocarditis in rats. *Infect. Immun.* 37, 127–131. doi: 10.1128/iai.37.1.127-131.1982
- Highman, B., Altland, P. D., and Roshe, J. (1959). Staphylococcal endocarditis and glomerulonephritis in dogs. *Circ. Res.* 7, 982–987. doi: 10.1161/01.res.7.6.982
- Highman, B., Roshe, J., and Altland, P. D. (1956). Production of endocarditis with *Staphylococcus aureus* and *Streptococcus mitis* in dogs with aortic insufficiency. *Circ. Res.* 4, 250–256. doi: 10.1161/01.res.4.3.250
- Hoen, B., and Duval, X. (2013). Clinical practice. Infective endocarditis. *N. Engl. J. Med.* 368, 1425–1433.
- Hoer, V., Franz, M., Pletz, M. W., Diab, M., Niemann, S., Faber, C., et al. (2018). *S. aureus* endocarditis: clinical aspects and experimental approaches. *Int. J. Med. Microbiol.* 308, 640–652. doi: 10.1016/j.ijmm.2018.02.004
- Höök, M., and Foster, T. J. (2000). “Molecular basis of adherence of *staphylococcus aureus* to biomaterials,” in *Infections Associated with Indwelling Medical Devices*, eds F. A. Waldvogel and A. L. Bisno (Washington, D.C.: ASM Press), 27–39. doi: 10.1128/9781555818067.ch2
- Johnson, C. M., Bahn, R. C., and Fass, D. N. (1986). Experimental porcine infective endocarditis: description of a clinical model. *Vet. Pathol.* 23, 780–782. doi: 10.1177/030098588602300620
- Johnson, M., Cockayne, A., and Morrissey, J. A. (2008). Iron-regulated biofilm formation in *Staphylococcus aureus* Newman requires ica and the secreted protein Emp. *Infect. Immun.* 76, 1756–1765. doi: 10.1128/iai.01635-07
- Jones, J. E. (1969). The experimental production of streptococcal endocarditis in the pig. *J. Pathol.* 99, 307–318. doi: 10.1002/path.1710990406
- Jones, J. E. T. (1982). Experimental streptococcal endocarditis in the pig: the development of lesions 18 to 48 hours after inoculation. *J. Comp. Pathol.* 92, 301–308. doi: 10.1016/0021-9975(82)90089-5
- Joost, I., Blass, D., Burian, M., Goerke, C., Wolz, C., von Müller, L., et al. (2009). Transcription analysis of the extracellular adherence protein from *Staphylococcus aureus* in authentic human infection and *in vitro*. *J. Infect. Dis.* 199, 1471–1478. doi: 10.1086/598484
- Juuti, K. M., Sinha, B., Werbick, C., Peters, G., and Kuusela, P. I. (2004). Reduced adherence and host cell invasion by methicillin-resistant *Staphylococcus aureus* expressing the surface protein Pls. *J. Infect. Dis.* 189, 1574–1584. doi: 10.1086/383348
- Kalinka, J., Hachmeister, M., Geraci, J., Sordelli, D., Hansen, U., Niemann, S., et al. (2014). *Staphylococcus aureus* isolates from chronic osteomyelitis are characterized by high host cell invasion and intracellular adaptation, but still induce inflammation. *Int. J. Med. Microbiol.* 304, 1038–1049. doi: 10.1016/j.ijmm.2014.07.013
- Kazlouskaya, V., Malhotra, S., Lambe, J., Idriss, M. H., Elston, D., and Andres, C. (2013). The utility of elastic Verhoeff-Van Gieson staining in dermatopathology. *J. Cutan. Pathol.* 40, 211–225. doi: 10.1111/cup.12036
- Kobayashi, S. D., Malachowa, N., and DeLeo, F. R. (2015). Pathogenesis of *Staphylococcus aureus* abscesses. *Am. J. Pathol.* 185, 1518–1527. doi: 10.1016/j.ajpath.2014.11.030
- Kolar, S. L., and Liu, G. Y. (2016). Targeting bacterial abscess formation. *EBioMedicine* 12, 16–17. doi: 10.1016/j.ebiom.2016.10.017
- Kreitmann, L., Moutagne, D., Launay, D., Morell-Dubois, S., Maillard, H., Lambert, M., et al. (2020). Clinical characteristics and outcome of patients with infective endocarditis diagnosed in a department of internal medicine. *J. Clin. Med.* 9:864. doi: 10.3390/jcm9030864
- Lam, T.-T., Giese, B., Chikkaballi, D., Kuhn, A., Wolber, W., Pane-Farre, J., et al. (2010). Phagolysosomal integrity is generally maintained after *Staphylococcus aureus* invasion of nonprofessional phagocytes but is modulated by strain 6850. *Infect. Immun.* 78, 3392–3403. doi: 10.1128/iai.00012-10
- Li, X., Wang, X., Thompson, C. D., Park, S., Park, W. B., and Lee, J. C. (2016). Preclinical efficacy of clumping factor A in prevention of *Staphylococcus aureus* infection. *mBio* 7:e02232-15.
- Liesenborghs, L., Meyers, S., Lox, M., Criel, M., Claes, J., Peetermans, M., et al. (2019). *Staphylococcus aureus* endocarditis: distinct mechanisms of bacterial adhesion to damaged and inflamed heart valves. *Eur. Heart J.* 40, 3248–3259. doi: 10.1093/eurheartj/ehz175
- Liesenborghs, L., Verhamme, P., and Vanassche, T. (2018). *Staphylococcus aureus*, master manipulator of the human hemostatic system. *J. Thromb. Haemost.* 16, 441–454. doi: 10.1111/jth.13928
- Mainiero, M., Goerke, C., Geiger, T., Gonser, C., Herbert, S., and Wolz, C. (2010). Differential target gene activation by the *Staphylococcus aureus* two-component system saeRS. *J. Bacteriol.* 192, 613–623. doi: 10.1128/jb.01242-09
- Maira-Litrán, T., Kropec, A., Abeygunawardana, C., Joyce, J., Mark, G., Goldmann, D. A., et al. (2002). Immunochemical properties of the staphylococcal poly-N-acetylglucosamine surface polysaccharide. *Infect. Immun.* 70, 4433–4440. doi: 10.1128/iai.70.8.4433-4440.2002
- Manandhar, S., Singh, A., Varma, A., Pandey, S., and Shrivastava, N. (2018). Evaluation of methods to detect *in vitro* biofilm formation by staphylococcal clinical isolates. *BMC Res. Notes* 11:714. doi: 10.1186/s13104-018-3820-9
- McDevitt, D., and Foster, T. J. (1995). Variation in the size of the repeat region of the fibrinogen receptor (clumping factor) of *Staphylococcus aureus* strains. *Microbiology* 141(Pt 4), 937–943. doi: 10.1099/13500872-141-4-937
- Mehta, R., Athar, M., Girgis, S., Hassan, A., and Becker, R. C. (2019). Acquired Von Willebrand Syndrome (AVWS) in cardiovascular disease: a state of the art review for clinicians. *J. Thromb. Thrombolysis* 48, 14–26. doi: 10.1007/s1239-019-01849-2
- Moreillon, P., Que, Y. A., and Bayer, A. S. (2002). Pathogenesis of streptococcal and staphylococcal endocarditis. *Infect. Dis. Clin. North Am.* 16, 297–318. doi: 10.1016/s0891-5520(01)00009-5
- Novick, R. P. (2003). Autoinduction and signal transduction in the regulation of staphylococcal virulence. *Mol. Microbiol.* 48, 1429–1449. doi: 10.1046/j.1365-2958.2003.03526.x
- O’Grady, N. P., Alexander, M., Dellinger, E. P., Gerberding, J. L., Heard, S. O., Maki, D. G., et al. (2002). Guidelines for the prevention of intravascular catheter-related infections. *Clin. Infect. Dis.* 35, 1281–1307.
- Pant, J., Goudie, M. J., Chaji, S. M., Johnson, B. W., and Handa, H. (2018). Nitric oxide releasing vascular catheters for eradicating bacterial infection. *J. Biomed. Mater. Res. B Appl. Biomater.* 106, 2849–2857. doi: 10.1002/jbm.b.34065
- Pappelbaum, K. I., Gorzelanny, C., Grässle, S., Suckau, J., Laschke, M. W., Bischoff, M., et al. (2013). Ultralarge von Willebrand factor fibers mediate luminal *Staphylococcus aureus* adhesion to an intact endothelial cell layer

- under shear stress. *Circulation* 128, 50–59. doi: 10.1161/circulationaha.113.002008
- Ring, J., Hoerr, V., Tuchscher, L., Kuhlmann, M. T., Löffler, B., Faber, C., et al. (2014). MRI visualization of *Staphylococcus aureus*-induced infective endocarditis in mice. *PLoS One* 9:e107179. doi: 10.1371/journal.pone.0107179
- Roberts, J. C., Krueger, R. L., Peak, K. K., Veguilla, W., Cannons, A. C., Amuso, P. T., et al. (2006). Community-associated methicillin-resistant *Staphylococcus aureus* epidemic clone USA300 in isolates from Florida and Washington. *J. Clin. Microbiol.* 44, 225–226. doi: 10.1128/jcm.44.1.225-226.2006
- Rowlands, D. T., Vakizadeh, J., Sherwood, B. F., and LeMay, J. C. (1970). Experimental bacterial endocarditis in the opossum (*Didelphis virginiana*). I. Valvular changes following a single injection of bacteria in unmodified adult opossums. *Am. J. Pathol.* 58, 295–304.
- Sadler, J. E. (1998). Biochemistry and genetics of von Willebrand factor. *Annu. Rev. Biochem.* 67, 395–424. doi: 10.1146/annurev.biochem.67.1.395
- Sande, M. A., and Zak, O. (1999). *Handbook of Animal Models of Infection: Experimental Models in Antimicrobial Chemotherapy*. San Diego, CA: Academic Press.
- Sause, W. E., Copin, R., O'malley, A., Chan, R., Morrow, B. J., Buckley, P. T., et al. (2017). *Staphylococcus aureus* strain Newman D2C contains mutations in major regulatory pathways that cripple its pathogenesis. *J. Bacteriol.* 199:e00476–17.
- Seidl, K., Bayer, A. S., McKinnell, J. A., Ellison, S., Filler, S. G., and Xiong, Y. Q. (2011). *In vitro* endothelial cell damage is positively correlated with enhanced virulence and poor vancomycin responsiveness in experimental endocarditis due to methicillin-resistant *Staphylococcus aureus*. *Cell. Microbiol.* 13, 1530–1541. doi: 10.1111/j.1462-5822.2011.01639.x
- Seidl, K., and Zinkernagel, A. S. (2013). The MTT assay is a rapid and reliable quantitative method to assess *Staphylococcus aureus* induced endothelial cell damage. *J. Microbiol. Methods* 92, 307–309. doi: 10.1016/j.mimet.2012.12.018
- Shrum, B., Anantha, R. V., Xu, S. X., Donnelly, M., Haeryfar, S. M. M., McCormick, J. K., et al. (2014). A robust scoring system to evaluate sepsis severity in an animal model. *BMC Res. Notes* 7:233. doi: 10.1186/1756-0500-7-233
- Singer, M., Deutschman, C. S., Seymour, C. W., Shankar-Hari, M., Annane, D., Bauer, M., et al. (2016). The third international consensus definitions for sepsis and septic shock (Sepsis-3). *JAMA* 315, 801–810.
- Starke, R. D., Ferraro, F., Paschalaki, K. E., Dryden, N. H., McKinnon, T. A. J., Sutton, R. E., et al. (2011). Endothelial von Willebrand factor regulates angiogenesis. *Blood* 117, 1071–1080.
- Strobel, M., Pförtner, H., Tuchscher, L., Völker, U., Schmidt, F., Kramko, N., et al. (2016). Post-invasion events after infection with *Staphylococcus aureus* are strongly dependent on both the host cell type and the infecting *S. aureus* strain. *Clin. Microbiol. Infect.* 22, 799–809. doi: 10.1016/j.cmi.2016.06.020
- Subedi, S., Jennings, Z., and Chen, S. C.-A. (2017). Laboratory approach to the diagnosis of culture-negative infective endocarditis. *Heart Lung Circ.* 26, 763–771. doi: 10.1016/j.hlc.2017.02.009
- Surewaard, B. G. J., Thanabalasuriar, A., Zeng, Z., Tkaczyk, C., Cohen, T. S., Bardeol, B. W., et al. (2018). α -toxin induces platelet aggregation and liver injury during *Staphylococcus aureus* sepsis. *Cell Host Microbe* 24, 271–284.e3. doi: 10.1016/j.chom.2018.06.017
- Traber, K. E., Lee, E., Benson, S., Corrigan, R., Cantera, M., Shopsin, B., et al. (2008). *agr* function in clinical *Staphylococcus aureus* isolates. *Microbiology* 154, 2265–2274.
- Tuchscher, L., Medina, E., Hussain, M., Völker, W., Heitmann, V., Niemann, S., et al. (2011). *Staphylococcus aureus* phenotype switching: an effective bacterial strategy to escape host immune response and establish a chronic infection. *EMBO Mol. Med.* 3, 129–141. doi: 10.1002/emmm.201000115
- Vandenesch, F., Lina, G., and Henry, T. (2012). *Staphylococcus aureus* hemolysins, bi-component leukocidins, and cytolytic peptides: a redundant arsenal of membrane-damaging virulence factors? *Front. Cell. Infect. Microbiol.* 2:12. doi: 10.3389/fcimb.2012.00012
- Vann, J. M., and Proctor, R. A. (1987). Ingestion of *Staphylococcus aureus* by bovine endothelial cells results in time- and inoculum-dependent damage to endothelial cell monolayers. *Infect. Immun.* 55, 2155–2163. doi: 10.1128/iai.55.9.2155-2163.1987
- Veloso, T. R., Amiguet, M., Rousson, V., Giddey, M., Vouillamoz, J., Moreillon, P., et al. (2011). Induction of experimental endocarditis by continuous low-grade bacteremia mimicking spontaneous bacteremia in humans. *Infect. Immun.* 79, 2006–2011. doi: 10.1128/iai.01208-10
- von Eiff, C., Heilmann, C., and Peters, G. (1999). New aspects in the molecular basis of polymer-associated infections due to staphylococci. *Eur. J. Clin. Microbiol. Infect. Dis.* 18, 843–846. doi: 10.1007/s100960050417
- Werdan, K., Dietz, S., Löffler, B., Niemann, S., Bushnaq, H., Silber, R. E., et al. (2014). Mechanisms of infective endocarditis: pathogen-host interaction and risk states. *Nat. Rev. Cardiol.* 11, 35–50. doi: 10.1038/nrcardio.2013.174
- Xie, Y., Tu, B., Xu, Z., Zhang, X., Bi, J., Zhao, M., et al. (2017). Bacterial distributions and prognosis of bloodstream infections in patients with liver cirrhosis. *Sci. Rep.* 7:11482.
- Zimmerli, W., Waldvogel, F. A., Vaudaux, P., and Nydegger, U. E. (1982). Pathogenesis of foreign body infection: description and characteristics of an animal model. *J. Infect. Dis.* 146, 487–497. doi: 10.1093/infdis/146.4.487

Conflict of Interest: The authors declare that the research was conducted in the absence of any commercial or financial relationships that could be construed as a potential conflict of interest.

Copyright © 2020 Schwarz, Hoerr, Töre, Hösker, Hansen, Van de Vyver, Niemann, Kuhlmann, Jeibmann, Wildgruber and Faber. This is an open-access article distributed under the terms of the Creative Commons Attribution License (CC BY). The use, distribution or reproduction in other forums is permitted, provided the original author(s) and the copyright owner(s) are credited and that the original publication in this journal is cited, in accordance with accepted academic practice. No use, distribution or reproduction is permitted which does not comply with these terms.